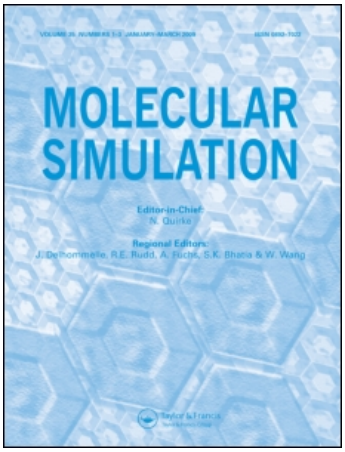

Molecular Simulation
Publication details, including instructions for authors and subscription information:
http://www.informaworld.com/smpp/title~content=t713644482

A Computer Simulation and Investigation of Liquid-Solid Interfacial Phenomena for Ice and Clathrate Hydrates

Ronald M. Pratt[a]; E. Dendy Sloan Jr[a]
[a] Chemical Engineering and Petroleum Refining Colorado School of Mines Golden, Colorado, USA

To cite this Article Pratt, Ronald M. and Sloan Jr, E. Dendy(1995) 'A Computer Simulation and Investigation of Liquid-Solid Interfacial Phenomena for Ice and Clathrate Hydrates', Molecular Simulation, 15: 4, 247 — 264
To link to this Article: DOI: 10.1080/08927029508022338
URL: http://dx.doi.org/10.1080/08927029508022338

Molecular Simulation, 1995, Vol. 15, pp. 247–264
Reprints available directly from the publisher
Photocopying permitted by license only

A COMPUTER SIMULATION AND INVESTIGATION OF LIQUID-SOLID INTERFACIAL PHENOMENA FOR ICE AND CLATHRATE HYDRATES

RONALD M. PRATT and E. DENDY SLOAN, Jr

Chemical Engineering and Petroleum Refining Colorado School of Mines Golden, Colorado 80401, USA

(Received February 1994, accepted January 1995)

Molecular dynamics has been employed to model the interface between liquid water and ice, liquid water and Structure I clathrate hydrates, and liquid water and Structure II clathrate hydrates. It has been found that the interfacial behavior between liquid water and ice and liquid water and hydrate crystal are qualitatively similar to each other and span a region of several molecular diameters on either side of the interface. Orientational and translational motion in the liquid is more vibrational in the interfacial region while temperature profiles are uniform across the interface. In addition, there was little tendency in any of the systems for the molecules in the liquid near the interface to arrange themselves in a more lattice-like structure. The exception to this was the hydration effect associated with exposed hydrocarbon molecules at the hydrate- water interface. The center of mass positions of molecules in the solid near the interface were somewhat perturbed.

KEY WORDS: Hydrates, interfaces, water

1 INTRODUCTION

Clathrate hydrates are formed when water molecules arrange themselves in a cage like structure around light hydrocarbon molecules. The resulting solid compounds resemble ice in their physical appearance. Clathrate hydrates naturally occur under conditions of high pressure and low temperature. Clathrate hydrates, subsequently referred to as hydrates were discovered in the laboratory by Sir Humphrey Davy [1] in 1811 and remained little more than a curiosity until 1934 [2] when they were observed as compounds occurring in pipelines.

The formation of clathrate hydrates and subsequent blockage of gas pipelines comprises a major industrial expense, both in terms of prevention, and in shutdown cost. It is desired to develop kinetic inhibitors which prevent the agglomeration of hydrates and thereby prevent blockage while at the same time being less expensive than the currently used thermodynamic inhibitors. This requires a molecular understanding of hydrate formation and of various inhibition mechanisms involving polymers, polypeptides, and surfactants. One initial step in such a work is to set up a computer simulation of ice and clathrate hydrates and to simulate their interfaces with liquid water. This model will then serve as a starting point from which one may investigate the effects of potential kinetic hydrate inhibitors.

The structural data for hydrates was determined by von Stackelberg [3] and these data provide input data for the hydrate simulation program. Structure I hydrates are made up of two kinds of cavities, i.e., two basic building blocks. These cavities, the 5^{12} cavity and the $5^{12}6^2$ cavity are shown in Figure 1. The nomenclature designates the first cage as containing 12 pentagonal faces and the latter as containing 12 pentagonal faces and 2 hexagonal faces. Similarly, Structure II hydrates are comprised of two building blocks, the 5^{12} cavity mentioned above, and the $5^{12}6^4$ cavity, also shown in Figure 1. The unit cells for these two hydrate structures are shown in Figure 2. The Structure I unit cell is cubic at 12 Å per side and contains 46 water molecules and 8 guest molecules. The Structure II unit cell is cubic at 17.3 Å per side and consists of 136 water molecules and 24 guest molecules. A comprehensive review of current hydrate research is found in a recent monograph by Sloan [4].

Comprehensive investigations of liquid water have been made by Stillinger [5, 6] and others. Molecular dynamics simulation has been performed for solid hydrates [7] and used to investigate the relative stability of the empty and filled hydrate lattice [8]. The ice-water interface has been investigated by molecular dynamics by Haymet and co-workers [9, 10]. In this work, three interfacial systems are investigated:

1. The Ice Ih–Water interface (for purposes of program verification and comparison with previous results);
2. The Structure I–Water interface;
3. The Structure II–Water interface.

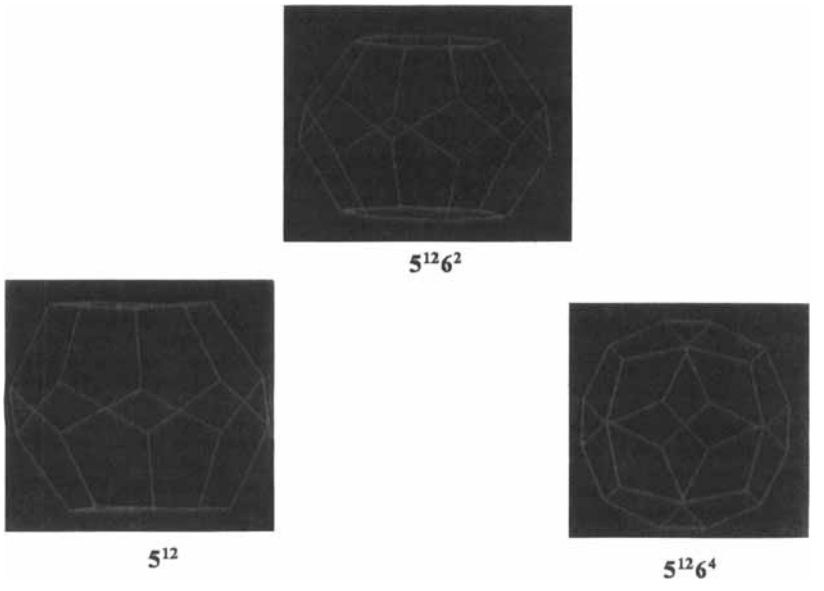

Figure 1 The Three Cavities found in structure I (5^{12} and $5^{12}6^2$) and Structure II (5^{12} and $5^{12}6^4$) Clathrate Hydrates. See Color Plate II.

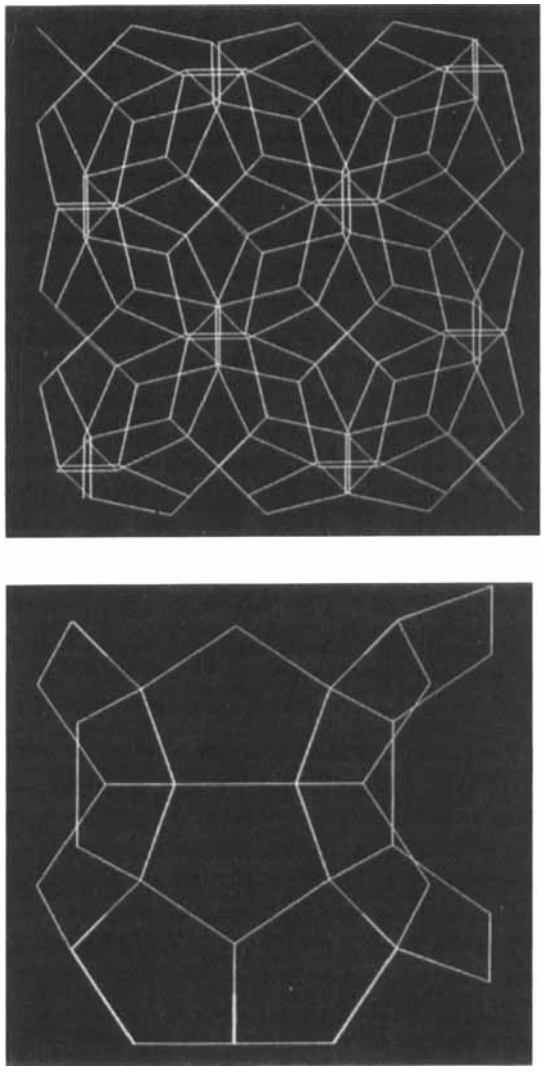

Figure 2 Unit Cells for Structure I and Structure II Clathrate Hydrates. See Color Plate III.

2 SIMULATION METHOD

The work of Karim and Haymet, [9, 10], which was later extended by Laird and Haymet, [11] and Haymet, [12] was used as a starting point in these solid–liquid interface studies. All of the simulations were done in the microcanonical (NVE) ensemble using the SPC model developed by Berendsen *et al.*, [13], and were set up as sandwiches with two layers of solid crystal separated by a layer of liquid water. The mean pressures were around 1 kbar $\pm$ 300 bar.

Each system contained two statistically independent interfaces so interfacial properties were averaged over both interfaces. Due to the sandwich layout of the systems, normal periodic boundary conditions could still be applied. These extremely large systems, which were on the order of a few thousand molecules, precluded the use of Ewald sums to calculate the electrostatic contributions to the potential, and hence, Ewald sums were not used. Cutoff distances of 9 Å were used for all simulations, i.e., molecular separations greater than 9 Å were not included in the calculation procedure.

All three systems were set up with the initial equilibrated system being entirely in the solid, crystalline phase. Velocities were then artifically scaled to very high temperatures (over 500 K) for the molecules in the middle of the sandwich, while the velocities of the molecules in the crystal lattice were held at 0 Kelvin. Within less than a few hundred femtoseconds the crystal lattice for the middle of the sandwich was destroyed. The simulations were allowed to continue to run for several tens of picoseconds to thoroughly destroy any remaining solid structure in the liquid phase.

After thorough melting, the central liquid section was then cooled to about 200 K and the artificial velocity constraints on the crystal were removed. A second equilibration was then necessary to relax the abruptly discontinuous interfaces. Equilibration consisted of 70 picoseconds for the ice–water interface and 300 picoseconds for the hydrate–water interfaces. Equilibrium criteria were:

1. Equipartition between translational and rotational energy;
2. Development of uniform velocity profiles (temperatures) across the interfaces;
3. No changes in average system pressure and configurational energy.

The shorter equilibration time was allowed for the ice–water system since published results were already observed. Energy drifts were compensated for by periodic velocity rescaling every 500–1000 picoseconds. Production runs for the ice–water interface were approximately 12 picoseconds. Subsequent production runs of equal duration did not show qualitatively different results. A production run of about 160 picoseconds was taken for the Structure I–water system and about 60 picoseconds for the significantly larger (see Table 2) Structure II–water system. In fact, interfacial phenomena were well developed within the first ten picoseconds.

In the case of the hydrate-water interfaces, it was also necessary to remove guest molecules from the melted liquid part of the interface to avoid abnormally high concentrations of apolar molecules in water. If these guest molecules were not removed, they would tend to aggregate together in a separate phase. These guest molecules were converted to water molecules by giving them appropriate charges, Lennard-Jones parameters, and non-zero quaternion values. In the case of the hydrate-water interface simulations, additional water molecules were added to the liquid phase so that the water density was identically 1.02 g/cc. Full occupancy, i.e., one guest molecule per cavity, was assumed for the hydrate phase.

The ice-water interfaces were simulated at about 200 ± 8 K and the hydrate-water interfaces were run at about 185 ± 8 K. Since the systems were run in the microcanonical ensemble, some fluctuation in the temperature could not be avoided. The reported melting point of SPC water is about 200 K [11]. The melting points of the hydrate crystals are unknown, so these systems were run at the lower temperature of about 185 K.

The ice–water interface was set up with cleavage perpendicular to the c axis. The system is shown in Figure 3. Table 1 gives the size and dimensions of each of the

Figure 3 The Ice–Water Interface. Yellow–Ice lattice, Red–Liquid water. See Color Plate IV.

ice–water interface systems. The water region thickness perpendicular to the interface was 70 Å in this case with ice Ih regions each of 23.3 Å giving the total simulation cell length of 116.7 Å.

Growth planes for clathrate hydrates are as yet unknown, and any plane which cleaves a hydrate structure will necessarily cut through a large number of cavities. The Structure I and Structure II interfaces are given in Figures 4 and 5 respectively. The ordered lattice structure is again easily distinguishable from the disordered liquid water. A summary of system sizes and dimensions is given in Table 2. The Structure *T*

Table 1 Ice–Water Interface System Size

	Box Dimensions (Å)	*Interfacial Area sq. (Å)*	*Simulation Cell Shape*	*Number of Water Molecules*
Figure 5-1	116.7 × 27.0 × 22.0	596	Parellepiped	2160

Figure 4 The Structure I Hydrates–Water Interface. White–Guest Molecules, Yellow–Structure I Hydrate Lattice, Red–Liquid. See Color Plate V.

Figure 5 The Structure II Hydrates–Water Interface. White–Guest Molecules, Yellow–Structure II Hydrate Lattice, Red–Liquid. See Color Plate VI.

simulation contains 128 guest molecules and the Structure II simulation contains 288 guest molecules. The thickness of the liquid region along an axis perpendicular to the interface for the Structure I system was 70.5 Å with end hydrate thicknesses of 23.5 Å, i.e., a total length of 117.5 Å for the simulation cell. For the Structure II- water interface system, the liquid region thickness was 67.4 Å with end hydrate thicknesses of 33.7 Å, giving a total length of 134.9 Å.

Table 2 Hydrate–Water Interface System Sizes

	Box Dimensions (Å)	*Interfacial Area sq. (Å)*	*Simulation Cell Shape*	*Number of Molecules*
Figure 5-4 (St.I)	23.5 × 117.5 × 23.5	552	Parellepiped	2184
Figure 5-5 (St.II)	33.7 × 134.9 × 33.7	1136	Parellepiped	5188

3 METHODS OF ANALYSIS

It was desired to observe behavior of the systems across the liquid-solid interface. This was done by dividing the system into a number of thin, parallel slices, with each slice parallel to the interface. Properties were then calculated for each slab, their values being a function of their distance from the interface. Following the work of Karim and Haymet, three properties were calculated, the oxygen density profile, dipole angle distribution, and translational mean square displacement. Two additional properties were determined, an orientational mean square displacement and an orientational autocorrelation function.

The oxygen density profile was obtained by dividing the system into a number of parallel slices about 0.2 Å thick. Each slab was parallel to the liquid-solid interface. The number of oxygen atoms located in each slab was then determined for each time step and averaged over the total simulation time. Lack of translational order is reflected by a nearly constant number of oxygen atoms from slice to slice. When crystalline order exists, the number of oxygen atoms per slice will vary in a definite, periodic pattern. The profile is very sensitive to small changes in the structure near the interface.

The distribution of dipole angles indicates whether the molecular orientation is ice-like or liquid-like. Slabs parallel to the interface were used, but about four angstroms in thickness. The dipole vector and its angle with the axis perpendicular to the interfacial plane was calculated for each molecule in the slab and averaged over the length of the simulation. The distribution is a sinusoidal curve for liquid water, but for solid ice, there are two distinct peaks. For the system shown in Figure 1, the peaks occur at 65° and 114°. This calculation for the solid ice crystal depends on the isotropic nature of the ice lattice, and is therefore not suitable for crystalline hydrates.

The translational mean square displacement gives an indication of how far a molecule has moved from its initial position. The mean square displacement is useful not only for distinguishing a liquid from a crystalline solid, but also in revealing the formation of a vitreous state. For a glass or a crystal, the molecules are fixed in their location. They will move about this fixed position, but they will not move away from their lattice site, i.e., the slope of the mean square displacement should be near zero; whereas, for a liquid, there will be a definite slope. The systems were divided into approximately four angstrom wide slabs, and the mean square displacement was determined for each slab.

The orientational mean square displacement quantity gives an indication of how much the orientation of a molecule has varied from its initial position. It is calculated the same way as the translational mean square displacement, but uses the four quaternion values, ζ, η, χ, ξ, [14, 15], with the constraint that the sum of the squares is

unity. For a crystalline solid, hydrogen bonding holds the molecules in a fixed orientation. There is orientational motion, but it is of a vibrational nature and the slope of the orientational mean square displacement curve is zero. For water in the liquid state, the orientation of the molecules is unrestricted and the curve will have a finite slope.

The autocorrelation function, defined as

$$C(t) = \langle A(t_0)A(t_0 + t)\rangle$$

[16], measures how a quantity at $t = t_0 + t$ is correlated with its value at t_0. The tendency of a molecule to "remember" its initial orientation can be determined by calculating the autocorrelation function of the quaternions or functions of the quaternions. The sum of three values from the second column of the matrix used to convert from body-fixed to space-fixed coordinates is used:

$$\begin{bmatrix} D_{xx} \\ D_{yy} \\ D_{zz} \end{bmatrix} = \begin{bmatrix} A_{11} & A_{21} & A_{31} \\ A_{12} & A_{22} & A_{23} \\ A_{13} & A_{23} & A_{33} \end{bmatrix} \begin{bmatrix} C_{xx} \\ C_{yy} \\ C_{zz} \end{bmatrix}$$

where the **D** matrix represents the body fixed atomic offsets from the center of mass, and the **C** matrix represents the space or laboratory fixed center of mass offsets. The entries of matrix **A** are functions of the four quaternion values [14]. The values of interest for the autocorrelation function, i.e., the second column of the matrix, are as follows:

$$A_{21} = -2^*(\xi\eta + \zeta\chi)$$

$$A_{22} = \xi^2 - \eta^2 - \zeta^2 + \chi^2$$

$$A_{23} = 2^*(\eta\chi - \xi\zeta)$$

The autocorrelation function is normalized so that values near unity indicate strong correlation between the orientation at time, t and the initial orientation. Departure from unity indicates the molecule's current orientation is independent of its starting value.

4 RESULTS

The oxygen density profiles for the ice-water interface and the two hydrate interfaces are shown in Figures 6–8 respectively. Common to all three systems was that interfacial disorder extended on the order of 10 Å into the solid phase; the liquid imposed a degree of translational disorder on the solid. There was no tendency for water molecules in the liquid to arrange in an ice- like lattice configuration in Figure 6. In Figures 7 and 8, however, there is some degree of order imposed in the liquid immediately adjacent to the interface. This is due to the hydration effects of the guest molecules at the interface; i.e., the apolar molecules existing in severed cages at the interface tend to draw water molecules from the liquid to complete their coordination shell.

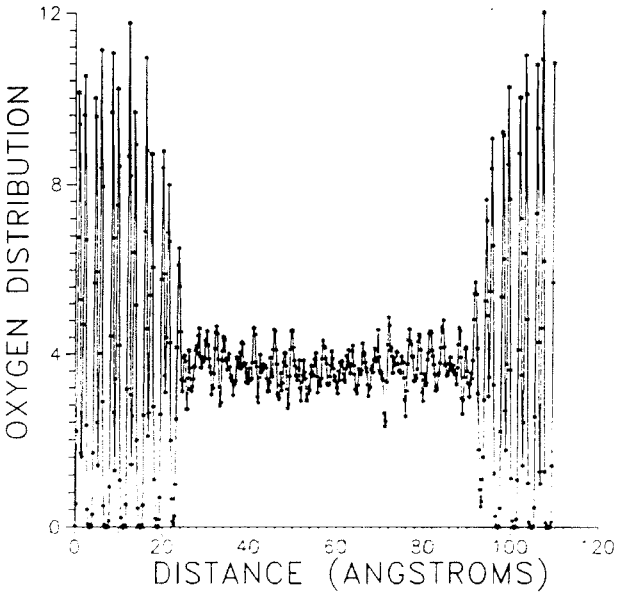

Figure 6 Oxygen Density Profile for Ice–Water Interface.

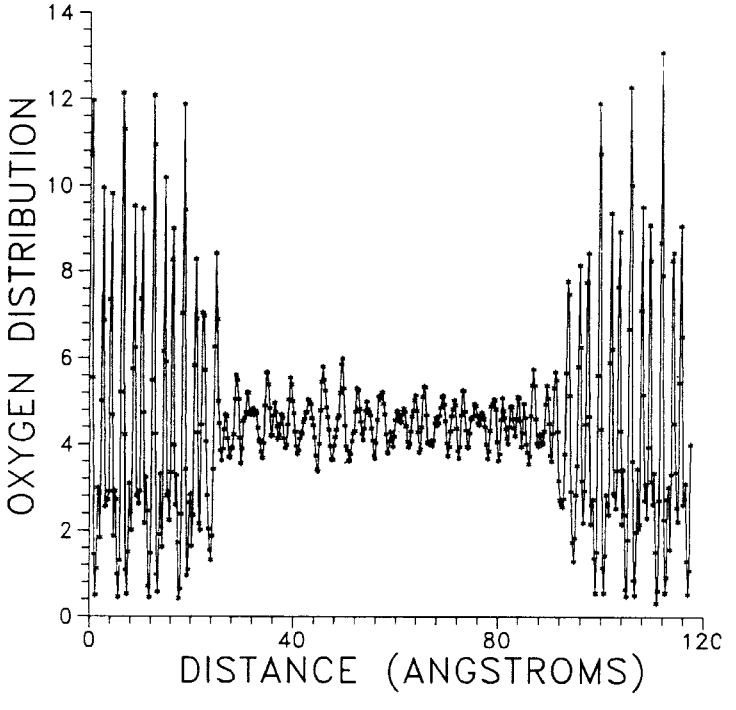

Figure 7 Oxygen Density Profile for Structure I Hydrates–Water Interface.

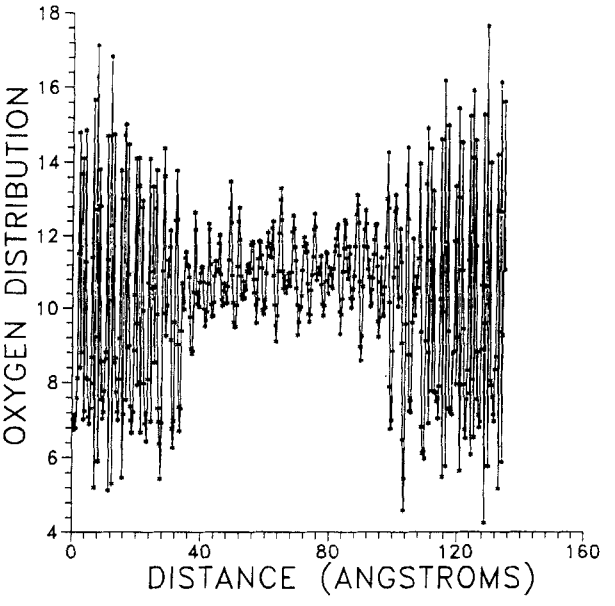

Figure 8 Oxygen Density Profile for Structure II Hydrates–Water Interface.

The remaining results for the interfaces were calculated for slabs of approximately four angstrom thickness. This includes the calculations for the dipole angle distribution, translational and orientational mean square displacements, and the orientational autocorrelation factor. As mentioned above, the symmetry of the interface models allowed for properties for the two interfaces to be averaged.

Tables 3–5 summarize the division scheme. A number inside the box indicates that data is presented for this slab and the numbers correspond to numbers on the following

Table 3 Data Presented for Ice–Water Interface, Cleavage 1

	1	2	3	4	5	6	7	8	9	10		

Table 4 Data Presented for Structure I Interface System

		1	2	3	4	5	6	7	8

Table 5 Data Presented for Structure II Interface System

1	2	3	4	5	6	7	8

figures. The heavy line indicates the theoretical interface between the solid (left) and liquid (right) phases.

Dipole angle distribution curves for the ice–water interface are shown in Figure 9. The double peaks correspond to solid ice and are normal distributions about the values mentioned above. The solid phase slab adjacent to the interface still shows the double peaks, but considerably reduced in magnitude. In addition, the value of the distribution at 90° is no longer zero. The liquid phase slab adjacent to the interface shows essentially the sinusoidal distribution characteristic of liquid water with a small dip at 90°. There are hence very small, but finite traces of orientational structure in the liquid. There is a much greater tendency, however, for molecules in the solid near the interface to orient themselves like liquid water than for the disordered molecules in the liquid phase to align themselves like the nearby solid.

Translational mean square displacements for the three interfacial systems are shown in Figures 10–12. Unlike the previous two features, the most notable interfacial perturbation is now found in the liquid phase. Molecules in the liquid near the interface are hindered in their motion for about 15 Å. Molecules in the solid phase immediately adjacent to the interface have no tendency to move in the ice–water interface. However, for the hydrate interfaces, there appears to be somewhat more motion of the solid-phase molecules next to the interface. A likely explanation for this is the severed cages mentioned above. A water molecule in a severed cage would be less stable than a water molecule in an ice lattice.

The orientational mean square displacements for the interface systems are shown respectively in Figures 13–15. Like translational motion, orientational motion is hindered as far as about 15 Å away from the interface into the liquid. The liquid phase

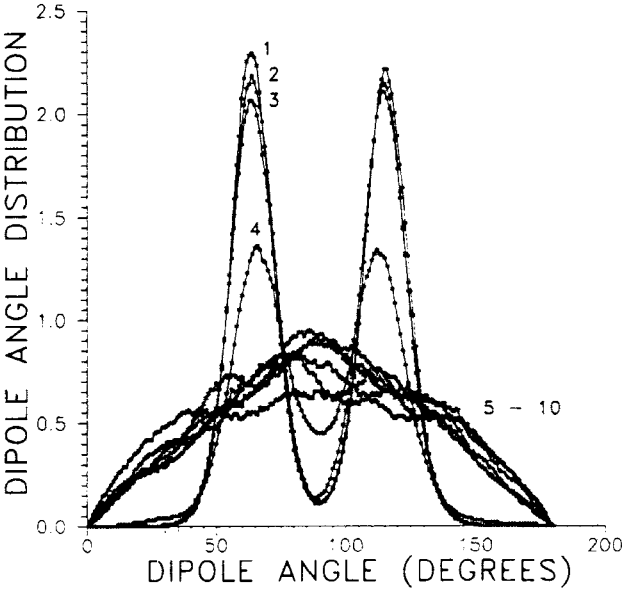

Figure 9 Dipole Angle Distribution for Ice–Water Interface.

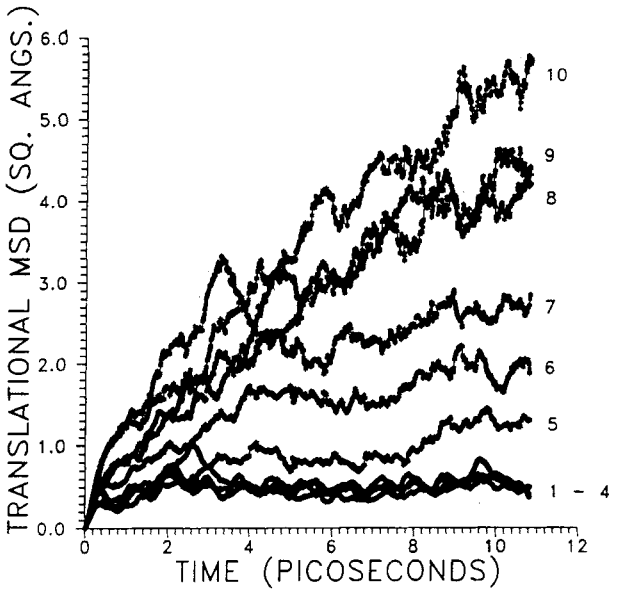

Figure 10 Translational Mean Square Displacement for Ice–Water Interface.

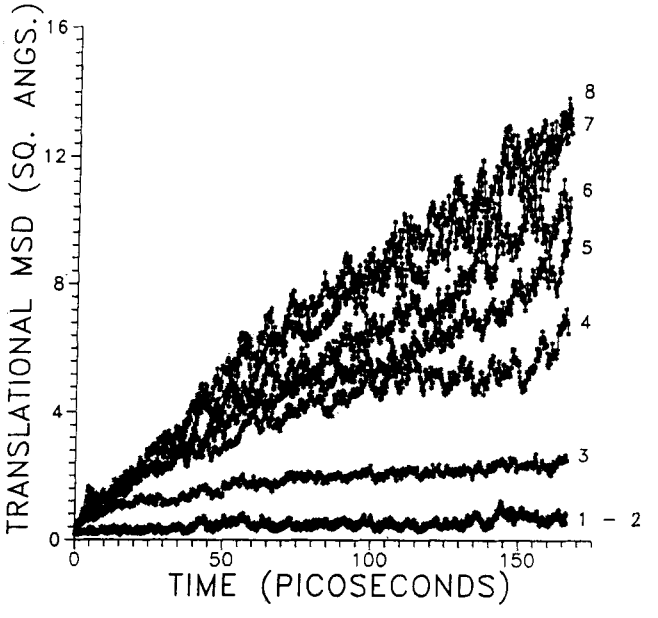

Figure 11 Translational Mean Square Displacement for Structure I Hydrates–Water Interface.

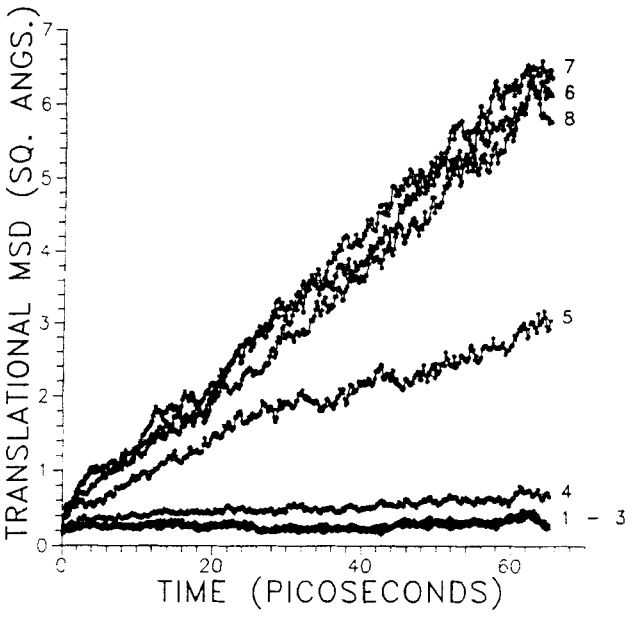

Figure 12 Translational Mean Square Displacement for Structure II Hydrates–Water Interface.

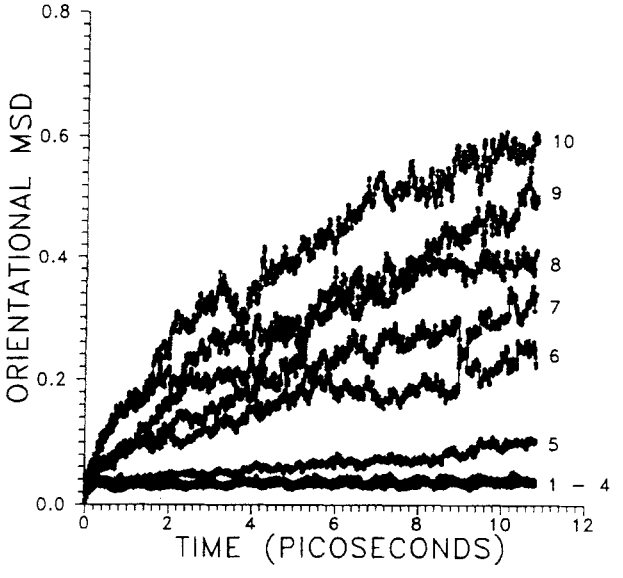

Figure 13 Orientational Mean Square Displacement for Ice–Water Interface.

molecules next to the ice in Figure 13 move scarcely more than their neighbors in the solid. In the hydrate systems there was orientational displacement of the molecules in the solid slab adjacent to the interface. The slopes of these curves (curve 3 in Figure 14, curve 4 in Figure 15) are near zero after about 50 picoseconds.

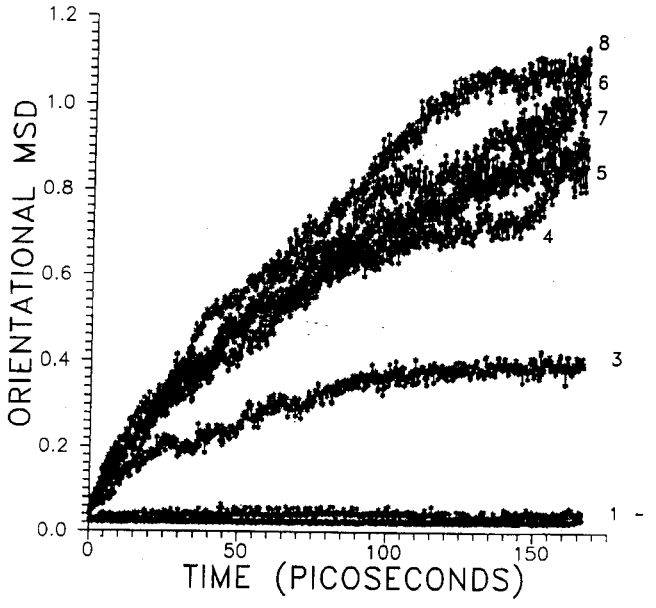

Figure 14 Orientational Mean Square Displacement for Structure I Hydrates–Water Interface.

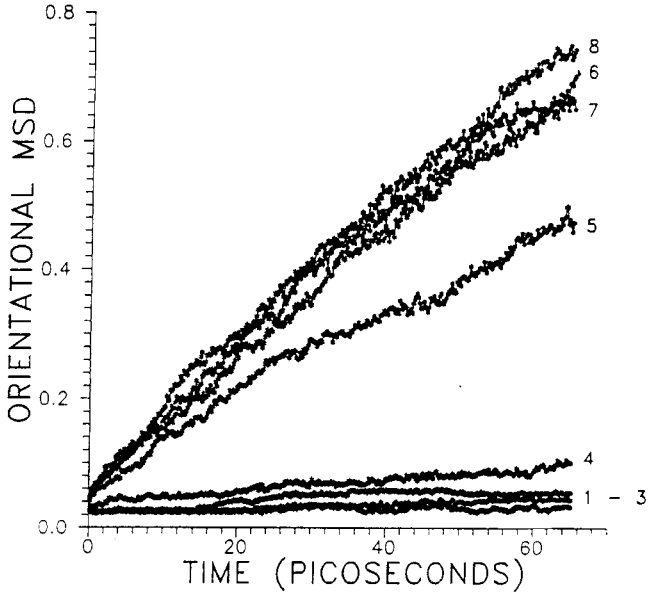

Figure 15 Orientational Mean Square Displacement for Structure II Hydrates–Water Interface.

Figures 16–18 give the autocorrelation factors for the respective systems. A value of unity implies that the average orientation of the molecules is dependent upon the initial orientation. This is observed for molecules in the solid region. The liquid phases show a steady decline in the autocorrelation factor, but this decay is very slow in the liquid

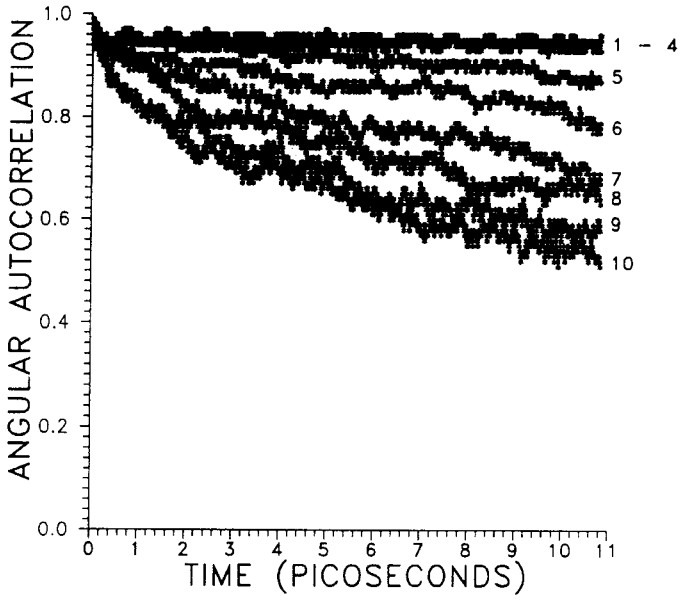

Figure 16 Orientational Autocorrelation Factor for Ice–Water Interface.

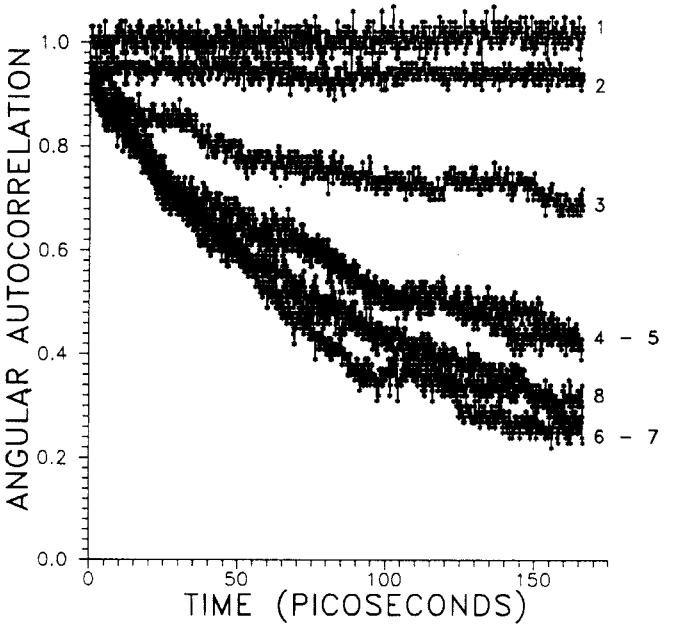

Figure 17 Orientational Autocorrelation Factor for Structure I Hydrates–Water Interface.

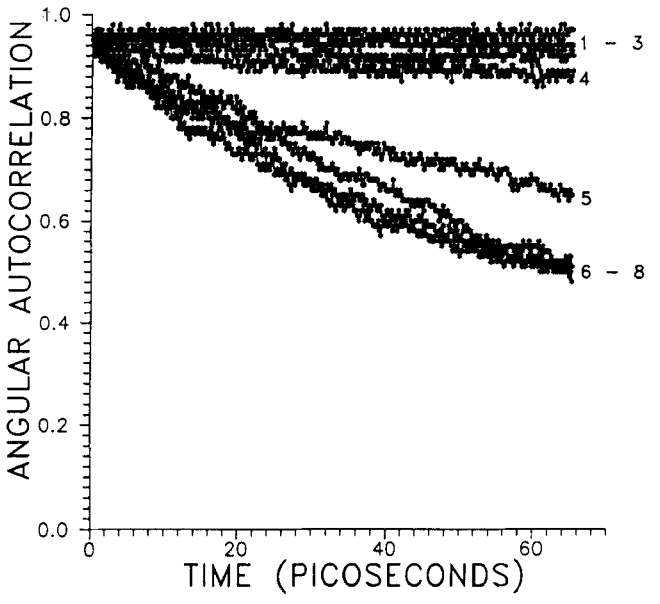

Figure 18 Orientational Autocorrelation Factor for Structure II Hydrates–Water Interface.

region next to the solid. The approximately 15 Å influence of the interface on the liquid is again observed. In the hydrate systems there was considerable orientational displacement of the molecules in the solid slab adjacent to the interface. The slopes of these curves (curve 3 in Figure 17, curve 4 in Figure 18) are near zero after about 50 picoseconds. This tendency is identical to that observed with the orientational mean square displacement.

5 CONCLUSIONS

The ice–water interface yields the same results of earlier studies and the hydrate-water interfaces behaved in a similar fashion:

1. The interface is actually a broad region spanning approximately 20–30 Å;
2. Orientational and translational disorder from the liquid phase penetrates the solid approximately 10–15 Å;
3. There is no imposition of structural order upon the liquid near the interface (with the exception of hydration effects associated with the hydrate interfaces);
4. Orientational and translational motion are hindered in the liquid near the interface as the motion becomes more vibrational; this extends 10–15 Å into the bulk liquid.

The fact that the liquid water adjacent to the interface has so little tendency to reconfigure itself in a lattice structure has implications on the reported difficulty of simulating the growth or formation of ordered structures from liquid water.

Acknowledgments

The authors wish to express appreciation to Dr. Raymond Mountain, NIST (Maryland) for providing a general water simulation program and to Professor Omar Karim, University of North Carolina (Wilmington) for aid in setting up the solid ice simulation. A Structure I hydrates simulation was performed by Dr. Jin Ping Long, Mobil (Dallas). Appreciation is also expressed to the Colorado School of Mines Hydrate Consortium for provision of computer facilities, and to the Amoco Foundation for their doctoral fellowship.

References

[1] H. Davy, "The Bakerian Lecture, On some of the Combinations of Oxymuriatic Gas and Oxygene, and on the Chemical Relations of these Principles to Inflammable Bodies", *Phil. Trans. Roy. Soc.* London, **101**, part I, 1 (1811).
[2] E. G. Hammerschmidt, "Formation of Gas Hydrates in Natural Gas Transmission Lines", *Ind. Eng. Chem.*, **26**, 851–5 (1934).
[3] H. R. Muller and M. von Stackelberg, "On the Structure of Gas Hydrates", *J. Chem. Phys.*, **19**, 1319–20 (1951).
[4] E. D. Sloan, *Clathrate Hydrates of Natural Gases*, Marcel Dekker, Inc., New York (1990).
[5] F. H. Stillenger, "Water Revisited", *Science*, **209**, 451 (1980).
[6] F. H. Stillenger and A. J. Rahman, "Improved Simulation of Liquid Water by Molecular Dynamics", *J. Chem. Phys.*, **60**, 1545 (1974).
[7] J. Tse, M. Klein and I. R. McDonald, "Molecular Dynamics Studies of Ice Ic and Structure I Clathrate of Methane", *J. Phys. Chem.*, **87**, 4198 (1983).
[8] P. Mark Rodger, "Stability of Gas Hydrates", *J. Phys. Chem.*, **94**, 6080–9 (1990).
[9] O. A. Karim and A. D. J. Haymet, "The Ice/Water Interface", *Chem. Phys. Let.*, **138** (6), 531 (1987).
[10] O. A. Karim and A. D. J. Haymet, "The Ice/Water Interface: A Molecular Dynamics Simulation Study", *J. Chem. Phys.*, **89** (11) 6889 (1988).
[11] B. B. Laird and A. D. J. Haymet, "The Crystal/Liquid Interface: Structure and Properties from Computer Simulation", *Chem. Rev.* **92**, 1819 (1992).
[12] A. D. J. Haymet, "Solvation, Freezing, and the Crystal/Liquid Interface: Modern Theories and Computer Simulation", *Fluid Phase Equilibria*, **83**, 415 (1993).
[13] H. Berendsen, J. Postma, W. von Gunstaren and J. Hermans, in *Intermolecular Forces*, edited by B. Pullman (Riedel, Dordrecht, Holland), 331 (1981).
[14] Evans, D. J., "On the Representation of Orientation Space", *Mol. Phys.*, **34**, 317 (1977).
[15] Evans, D. J. and Murad, S. "Singularity free Algorithm for Molecular Dynamics Simulation of Rigid Polyatomics", *Mol. Phys.*, **34**, 327 (1977).
[16] J. M. Haile, *Molecular Dynamics Simulation, Elementary Methods*, Wiley Interscience, New York, (1992).